

Empirical Constraints on Parton Energy Loss in Heavy-ion Collisions at the LHC

Thomas Marshall,^{1,*} Philip Suh,¹ Gang Wang,¹ and Huan Zhong Huang^{1,2}

¹*Department of Physics and Astronomy, University of California, Los Angeles, California 90095, USA*

²*Key Laboratory of Nuclear Physics and Ion-beam Application (MOE),
and Institute of Modern Physics, Fudan University, Shanghai-200433, People's Republic of China*

(Dated: October 3, 2023)

Energetic quarks and gluons lose energy as they traverse the hot and dense medium created in high-energy heavy-ion collisions at the BNL Relativistic Heavy Ion Collider (RHIC) and the CERN Large Hadron Collider (LHC). The nuclear modification factor (R_{AA}) of leading particles quantifies parton energy loss in such collisions, with the particle spectrum in $p+p$ collisions as a reference. Previous R_{AA} measurements at RHIC energies have revealed an approximately constant trend at high transverse momenta (p_T), implying a scenario where parton energy loss, Δp_T , scales proportionally with p_T , a feature naively expected from energy loss dynamics in elastic collisions. In this study, we investigate the LHC R_{AA} measurements which exhibit a pronounced p_T dependence of R_{AA} for various particle species, and our analysis attributes this behavior to Δp_T being approximately proportional to $\sqrt{p_T}$. These distinct features are consistent with model calculations of dominant radiative energy loss dynamics at the LHC, in contrast to the dominance of collisional energy loss at RHIC. Additionally, the linear increase of fractional energy loss with medium density at different p_T magnitudes affirms the previous empirical observation that the magnitude of the energy loss depends mostly on the initial entropy density, with no significant path length dependence. Implications on the dynamical scenarios of parton energy loss and future experimental investigations will also be discussed.

keywords: heavy-ion collision; nuclear modification factor; parton energy loss

Color opacity stands as a fundamental trait of the hot and dense medium created in heavy-ion collisions at the BNL Relativistic Heavy Ion Collider (RHIC) and the CERN Large Hadron Collider (LHC). As energetic quarks and gluons traverse the medium, they shed energy through elastic scattering [1–4] and radiation of soft gluons [5–7]. In the scenario of an infinitely-high-momentum parton, energy loss would predominantly occur through radiative processes. Conversely, in the opposite scenario, collisional energy loss would become the dominant factor. Prior empirical examinations of final-state leading particle spectra and the pertinent nuclear effects, using RHIC data, have revealed the proportionality between parton energy loss (Δp_T) and the magnitude of transverse momentum (p_T), supporting the prevalence of collisional energy loss [8]. Given that collision center-of-mass energies ($\sqrt{s_{NN}}$) at the LHC significantly surpass those at RHIC by over an order of magnitude, the associated p_T range of generated particles now spans into a realm where radiative energy loss dynamics are expected to assume a more prominent role. Hence, the analysis of LHC data using the same framework as in Ref. [8] is warranted to investigate the potential transition in the dynamics of energy loss from RHIC to the LHC.

Both radiative and collisional energy losses are intricately linked to the path length (L) and the entropy density of the medium. We approximate the medium entropy density as $\frac{1}{S} \frac{dN}{dy}$, where $\frac{dN}{dy}$ represents the experimentally measured particle density per unit rapidity,

and S corresponds to the transverse overlap area of the colliding system, which can be determined using Monte Carlo Glauber calculations [9–12]. A previous study of RHIC data has unraveled the lack of or minimal dependence of Δp_T on L , implying that parton energy loss is predominantly determined by the initial medium density [8]. This feature could arise from the scenario of rapid expansion of the collision system, resulting in a swift decrease in medium entropy density over time. It is of great interest to investigate whether the LHC data corroborate the same characteristics.

In experiments, the nuclear modification factor, R_{AA} , quantifies the suppression or enhancement of particle yields in heavy-ion collisions relative to a nucleon-nucleon (NN) reference:

$$R_{AA}(p_T) = \frac{d^2 N^{AA}/dp_T d\eta}{T_{AA} d^2 \sigma^{NN}/dp_T d\eta}, \quad (1)$$

where T_{AA} accounts for the nuclear collision geometry, and η denotes pseudorapidity. Both STAR [13][14] and PHENIX [15][16] data demonstrate a plateauing of the R_{AA} spectrum at values much lower than unity in the high- p_T region ($\gtrsim 5$ GeV/c). Treating the suppression of the nuclear modification factor as a result of empirical loss of transverse momentum from the $p+p$ spectrum to the nucleus+nucleus spectrum, these flat R_{AA} curves were found to indicate a constant fractional p_T shift in the spectrum. From a classical standpoint, this behavior is consistent with elastic collisional energy loss. Higher- p_T particles would lose a proportionally higher amount of momentum through elastic collisions within the medium, resulting in a constant $\Delta p_T/p_T$. While this seems to

* rosstom@g.ucla.edu

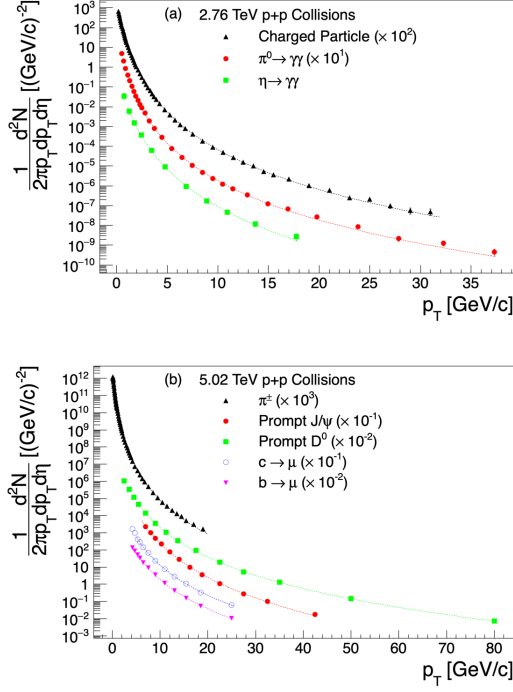


FIG. 1. Particle p_T spectra in $p+p$ collisions at (a) 2.76 TeV and (b) 5.02 TeV. The 2.76 TeV data (charged particles, π^0 , and η) are from ALICE [18, 19]. The 5.02 TeV results include charged pions from ALICE [20], prompt J/ψ and prompt D^0 mesons from CMS [21, 22], and muons from charm and bottom hadrons from ATLAS [23]. Different scaling factors are applied for better visibility. Fits to the data follow Eq. (2) as discussed in the text.

describe the observed RHIC data fairly well, LHC data demonstrate significantly different characteristics.

Figure 1 depicts the published p_T spectra of various final-state particles in $p+p$ collisions at (a) 2.76 TeV and (b) 5.02 TeV. Each dataset can be described by a Tsallis distribution [17]:

$$\frac{1}{2\pi p_T} \frac{d^2N}{dp_T dn} = A \left(1 + \frac{p_T}{p_0}\right)^{-n}, \quad (2)$$

where A , p_0 , and n are free parameters in the fit. Note that certain datasets have been adjusted by scaling factors compared to their original sources. These scaling factors will be incorporated into the parameter A and do not affect the relevant physics being investigated.

Following the procedures outlined in Ref. [8] and treating the suppression empirically as a horizontal shift in the p_T spectrum from $p+p$ to $A+A$ collisions, we can express R_{AA} as

$$R_{AA}(p_T) = \frac{(1 + p'_T/p_0)^{-n} p'_T}{(1 + p_T/p_0)^{-n} p_T} \left[1 + \frac{dS(p_T)}{dp_T}\right] \quad (3)$$

where $p'_T \equiv p_T + S(p_T)$, and $S(p_T)$ is the magnitude of the shift. Although $S(p_T)$ being proportional to p_T

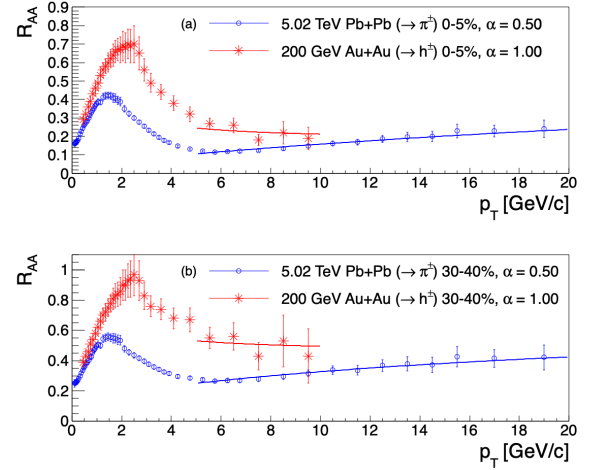


FIG. 2. R_{AA} as a function of p_T for charged hadrons in Au+Au collisions at 200 GeV (red) [13] and for charged pions in Pb+Pb collisions at 5.02 TeV (blue) [20] for (a) 0–5% and (b) 30–40% centrality ranges. The fit functions follow Eq. (4) with fixed α values of 1 and 0.5 for RHIC and the LHC data, respectively, using the corresponding p_0 and n values extracted from the Tsallis fits in Fig. 1.

adequately describes RHIC data at the high- p_T region, we start with a more general form in this paper, namely $S(p_T) = S_0 p_T^\alpha$. Then, Eq. (3) becomes

$$R_{AA}(p_T) = \frac{[1 + (p_T + S_0 p_T^\alpha)/p_0]^{-n} (p_T + S_0 p_T^\alpha)}{(1 + p_T/p_0)^{-n} p_T} \times (1 + S_0 \alpha p_T^{\alpha-1}). \quad (4)$$

Once we determine p_0 and n for each particle species from the p_T distribution in Fig. 1, we regard them as fixed parameters in Eq. (4), and use this formula to fit the corresponding R_{AA} data allowing S_0 and α to vary as free parameters.

The necessity of introducing the α parameter is convincingly illustrated in Fig. 2, which shows the R_{AA} measurements as a function of p_T for charged hadrons in Au+Au collisions at 200 GeV [13] and for charged pions in Pb+Pb collisions at 5.02 TeV [20] for (a) 0–5% and (b) 30–40% centrality ranges. The fit functions adhere to Eq. (4) with S_0 serving as the sole free parameter. At $p_T \gtrsim 5$ GeV/c, the flat R_{AA} patterns at RHIC agree with $\alpha = 1$, whereas the increasing trends at the LHC harmonize with $\alpha = 0.5$. At both collision energies, the flattening and increasing trends initiate at approximately the same p_T value of around 5 GeV/c. This pattern is also evident in the R_{AA} data for other particle species to be presented, presumably because below this p_T the soft physics dynamics including hydrodynamics and coalescence formation dominate, whereas above the p_T of 5 GeV/c parton fragmentation starts to dominate particle production where the parton energy loss picture emerges.

Figure 3 delineates $R_{AA}(p_T)$ for charged hadrons in (a) 0–5% and (b) 30–40% Pb+Pb collisions at 2.76 TeV [24],

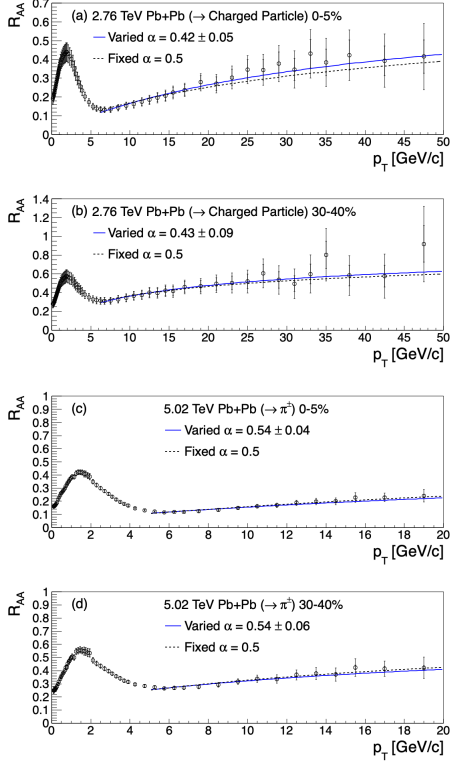


FIG. 3. $R_{AA}(p_T)$ for charged hadrons in (a) 0–5% and (b) 30–40% Pb+Pb collisions at 2.76 TeV [24], and for charged pions in (c) 0–5% and (d) 30–40% Pb+Pb collisions at 5.02 TeV [20]. The fit functions from Eq. (4) either take α as a free parameter or fix it at 0.5, using the p_0 and n values extracted from the Tsallis fits in Fig. 1.

and for charged pions in (c) 0–5% and (d) 30–40% Pb+Pb collisions at 5.02 TeV [20]. All the datasets exhibit upward trends for $p_T \gtrsim 5$ GeV/c. When we apply the same fitting approach and fix α at 0.5, the resulting fit curves (dashed lines) adequately capture all the data points. When we take α as a free parameter (solid curve), the extracted α values are consistent with 0.5 within statistical uncertainties.

We further investigate whether other final-state leading particles also exhibit these features. Figure 4 shows similar rising trends of R_{AA} at higher p_T for (a) π^0 and (b) η mesons in 0–10% Pb+Pb at 2.76 TeV [25], for (c) prompt J/ψ meson in 0–100% Pb+Pb at 5.02 TeV [21], and for (d) prompt D^0 meson in 0–10% Pb+Pb at 5.02 TeV [22]. The α values extracted for π^0 , η , and J/ψ mesons are consistent with 0.5 within the fitted statistical uncertainties. The fits to the prompt D^0 data seem to show some tension between the varied and fixed α values, but the difference is a less-than- 2σ effect. The curve with the fixed parameter ($\alpha = 0.5$) does appear to agree with all the data points within the uncertainties. More precise measurements of D^0 R_{AA} are required to better constrain the value of α .

Figure 5 displays $R_{AA}(p_T)$ for muons originating from

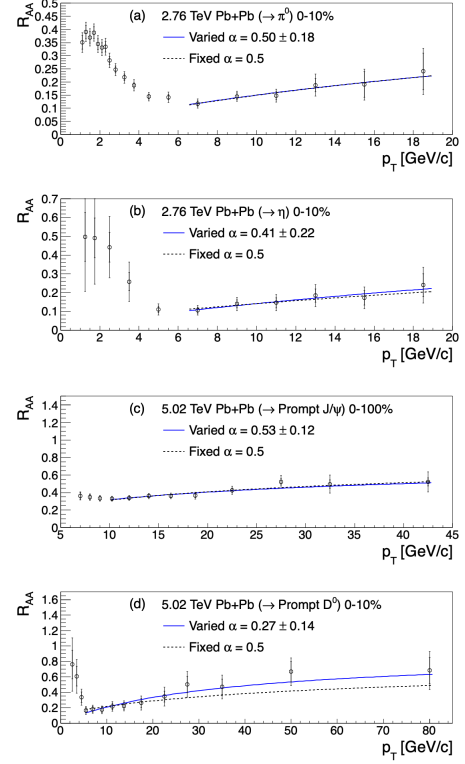


FIG. 4. $R_{AA}(p_T)$ for (a) π^0 and (b) η mesons in 0–10% Pb+Pb collisions at 2.76 TeV [25], for (c) prompt J/ψ mesons in 0–100% Pb+Pb collisions at 5.02 TeV [21], and for (d) prompt D^0 mesons in 0–10% Pb+Pb collisions at 5.02 TeV [22]. The fit functions from Eq. (4) either take α as a free parameter or fix it at 0.5, using the p_0 and n values extracted from the Tsallis fits in Fig. 1.

(a) charm and (b) bottom hadrons in 0–10% Pb+Pb collisions at 5.02 TeV. In both cases, the fit curves with $\alpha = 0.5$ align with all the data points within uncertainties. The α values extracted from the free-parameter fits exhibit a slight deviation from 0.5, with less than 1.5σ significance.

To recap, the analyzed LHC data here suggest that to explain the R_{AA} measurements for light- and heavy-quark hadrons as a p_T shift in the spectrum from $p+p$ collisions, we require the corresponding Δp_T to scale with $\sqrt{p_T}$. This p_T dependence contrasts with the previously observed proportionality with p_T in RHIC data. Our analysis results with more recent data are in line with a previous study of LHC R_{AA} data that determined the α value to be 0.55 [26]. Our p_T dependence of the parton energy loss at LHC supports theoretical predictions involving energy loss dynamics from medium-induced gluon radiation [27]. The distinct change from $\alpha = 1$ at RHIC to $\alpha = 0.5$ at LHC suggests a transition in the relative importance of collisional energy loss dynamics to radiative energy loss dynamics.

The transition in the parton energy loss dynamics in the medium might find an explanation in the VNI/BMS

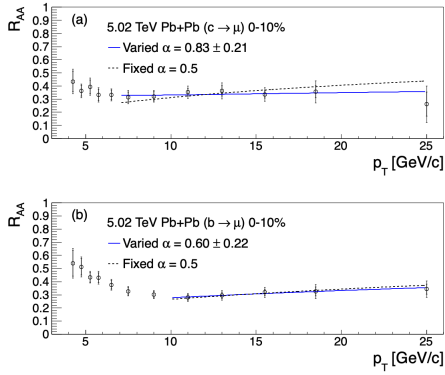


FIG. 5. $R_{AA}(p_T)$ for muons from (a) charm and (b) bottom hadrons in 0–10% Pb+Pb collisions at 5.02 TeV [23]. The fit functions from Eq. (4) either take α as a free parameter or fix it at 0.5, using the p_0 and n values extracted from the Tsallis fits in Fig. 1.

parton cascade model calculations [28] that propose a significant reduction in parton collisional energy loss as the medium mass scale increases. The substantially higher $\sqrt{s_{NN}}$ at the LHC leads to a considerably greater abundance of heavy quarks within the medium compared with RHIC. This increase in the medium mass scale could consequently cause a reduction in collisional energy loss. Another theoretical prediction, using the Monte Carlo pQCD tomographic model, known as CUJET1.0 [29], initially underestimates the growth of R_{AA} with p_T at LHC energies. In order to describe the LHC data, this model necessitates an adaptation that enhances the relative contribution of radiative energy loss over collisional energy loss at the LHC.

The VNI/BMS calculations for charm quark energy loss at RHIC energies agree with the prevailing collisional energy loss up until the 7–12 GeV/c region for initial charm quarks, followed by a crossover to the dominance of radiative energy loss and a plateauing effect at higher momenta [30]. Extending this investigation to LHC energies may offer insights into elucidating the subtle upward trend observed in the higher p_T range, especially in relation to the nuanced distinctions between heavy-quark and light-quark behaviors.

The dead-cone effect [31] predicts that gluon radiation is more strongly suppressed for bottom quarks than charm quarks, as the former bears a larger mass-to-energy ratio, leading to a wider dead cone. Recent measurements of heavy-quark meson production in $p+p$ collisions by the ALICE experiment [32] reveal heavy-quark fragmentation in the vacuum and provide a direct observation of the dead-cone effect. However, the LHC data of the R_{AA} trends for muons from charm and bottom decays do not exhibit the anticipated reduced radiative energy loss for bottom quarks. The decay muon measurements can be influenced by various factors, including substantial momentum smearing resulting from decay kinematics and the existence of non-prompt $c \rightarrow \mu$

decays that originate from b quarks. Another factor to consider is that the dead-cone effect may become less pronounced for very-high-energy quarks represented in the muon measurements. More precise data are needed to elucidate the nature of heavy-quark dynamics in the medium.

We also investigate the relationship between energy loss and path length at LHC energies. Previous examinations of RHIC data have revealed that the deduced fractional energy loss, $\Delta p_T/p_T$, is a linear function of medium initial entropy density (quantified by $\frac{1}{S} \frac{dN}{dy}$) across different centrality intervals, despite significant variations in the path length for traversing partons [8]. This suggests a weak dependence of energy loss on path length. We apply the same analysis to LHC data, and discover similar outcomes, as shown in Fig. 6. Now that fractional energy loss varies with p_T according to the LHC R_{AA} data, we plot $\Delta p_T/p_T$ as a function of $\frac{1}{S} \frac{dN}{dy}$ at different p_T values for charged hadrons in Pb+Pb collisions at 2.76 TeV and for charged pions in Pb+Pb collisions at 5.02 TeV. In each case for each p_T regime, a clear linear trend emerges, and the linearity is especially strong for higher p_T scales, where parton fragmentation dominates particle production. These findings support the earlier observation of a weak path length dependence of parton energy loss, even though the medium densities at RHIC and the LHC are very different. As discussed for RHIC data [8], the weak path length dependence of energy loss could arise from the rapid expansion of the medium, where the majority of energy loss occurs before the parton is able to traverse a full path length. Thereby, medium density becomes the dominant factor that determines the energy loss during the rapid expansion. We argue that in such a rapidly expansive medium, the static path length from the initial geometry of colliding nuclei fails to trace the parton energy loss in the medium.

In summary, we present a parton energy loss study showing a significant distinction between RHIC and LHC data when empirically interpreting $R_{AA}(p_T)$ as a momentum loss in $A+A$ collisions relative to the $p+p$ reference. While the RHIC data favor a direct proportionality between the p_T shift and p_T itself, the LHC data suggest a proportionality with $\sqrt{p_T}$. This difference in the p_T dependence signifies the heightened importance of radiative energy loss compared with collisional energy loss within the same transverse momentum range in colliding systems at higher $\sqrt{s_{NN}}$. Additionally, we find that the magnitude of the parton energy loss at LHC is largely determined by the initial medium entropy density, consistent with previous results at RHIC, indicating a limited path length dependence of parton energy loss, and placing greater emphasis on the initial medium density for a rapid explosive medium. The distinct parton energy loss dynamics at RHIC and at LHC can be further investigated with high-statistics heavy-quark-tagged jets from the sPHENIX at RHIC, as well as the LHC experiments in future runs.

ACKNOWLEDGMENTS

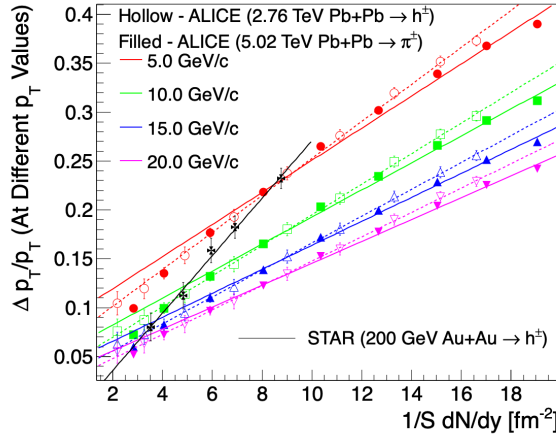


FIG. 6. Fractional energy loss ($\Delta p_T/p_T$) as a function of centrality (in terms of $\frac{1}{S} \frac{dN}{dy}$) based on the analysis in this study and Ref. [8] for charged hadrons in Au+Au collisions at 200 GeV [13] and in Pb+Pb at 2.76 TeV, and for charged pions in Pb+Pb at 5.02 TeV. Each of the LHC data points corresponds to a specific p_T value used to calculate fractional energy loss, whereas fractional energy loss has no p_T -dependence in RHIC data [8]. $\frac{1}{S} \frac{dN}{dy}$ values are calculated using the appropriate S_{\perp}^{var} and $\frac{dN}{dy}$ columns from Table I of Ref. [33]. Each data set is fit separately with a linear function.

The authors thank Dylan Neff, Jared Reiten, and Anthony Frawley for many fruitful discussions. T. M., P. S., G. W., and H. H. are supported by the U.S. Department of Energy under Grant No. DE-FG02-88ER40424 and by the National Natural Science Foundation of China under Contract No.1835002.

-
- [1] H. van Hees and R. Rapp, *Thermalization of heavy quarks in the quark-gluon plasma*, *Phys. Rev. C* **71** (Mar, 2005) 034907.
 - [2] G. D. Moore and D. Teaney, *How much do heavy quarks thermalize in a heavy ion collision?*, *Phys. Rev. C* **71** (Jun, 2005) 064904.
 - [3] M. G. Mustafa, *Energy loss of charm quarks in the quark-gluon plasma: Collisional vs radiative losses*, *Phys. Rev. C* **72** (Jul, 2005) 014905.
 - [4] A. Adil, M. Gyulassy, W. Horowitz and S. Wicks, *Collisional energy loss of nonasymptotic jets in a quark-gluon plasma*, *Phys. Rev. C* **75** (Apr, 2007) 044906.
 - [5] Y. L. Dokshitzer and D. E. Kharzeev, *Heavy quark colorimetry of QCD matter*, *Phys. Lett. B* **519** (2001) 199–206, [[hep-ph/0106202](#)].
 - [6] A. Adil and M. Gyulassy, *Energy systematics of jet tomography at rhic: $\sqrt{s}=62.4$ vs 200agev*, *Physics Letters B* **602** (2004) 52–59.
 - [7] I. Vitev, *Testing the theory of qgp-induced energy loss at rhic and the lhc*, *Physics Letters B* **639** (2006) 38–45.
 - [8] G. Wang and H. Z. Huang, *Empirical constraints on parton energy loss in nucleus–nucleus collisions at rhic*, *Physics Letters B* **672** (2009) 30–34.
 - [9] PHENIX collaboration, K. Adcox, S. S. Adler, N. N. Ajitanand, Y. Akiba, J. Alexander, L. Aphecetche et al., *Centrality dependence of charged particle multiplicity in au+au collisions at $\sqrt{s_{NN}}=130$ GeV*, *Phys. Rev. Lett.* **86** (Apr, 2001) 3500–3505.
 - [10] PHOBOS collaboration, B. B. Back, M. D. Baker, D. S. Barton, R. R. Betts, R. Bindel, A. Budzanowski et al., *Centrality dependence of charged particle multiplicity at midrapidity in au+au collisions at $\sqrt{s_{NN}}=130$ GeV*, *Phys. Rev. C* **65** (Feb, 2002) 031901.
 - [11] I. Bearden, D. Beavis, C. Besliu, Y. Blyakhman, J. Brzychczyk, B. Budick et al., *Charged particle densities from au+au collisions at $s_{nn}=130$ gev*, *Physics Letters B* **523** (2001) 227–233.
 - [12] STAR collaboration, B. I. Abelev, M. M. Aggarwal, Z. Ahammed, B. D. Anderson, D. Arkhipkin, G. S. Averichev et al., *Systematic measurements of identified particle spectra in pp, d + Au, and Au + Au collisions at the star detector*, *Phys. Rev. C* **79** (Mar, 2009) 034909.
 - [13] STAR collaboration, J. Adams et al., *Transverse momentum and collision energy dependence of high p(T) hadron suppression in Au+Au collisions at ultrarelativistic energies*, *Phys. Rev. Lett.* **91** (2003) 172302, [[nuc1-ex/0305015](#)].
 - [14] STAR collaboration, B. I. Abelev et al., *Transverse momentum and centrality dependence of high- p_T non-photonic electron suppression in Au+Au collisions at $\sqrt{s_{NN}}=200$ GeV*, *Phys. Rev. Lett.* **98** (2007) 192301, [[nuc1-ex/0607012](#)].
 - [15] PHENIX collaboration, S. S. Adler et al., *A Detailed Study of High-p(T) Neutral Pion Suppression and Azimuthal Anisotropy in Au+Au Collisions at $s(NN)^{(1/2)}=200$ -GeV*, *Phys. Rev. C* **76** (2007) 034904, [[nuc1-ex/0611007](#)].
 - [16] A. Adare, S. Afanasiev, C. Aidala, N. N. Ajitanand, Y. Akiba, H. Al-Bataineh et al., *Energy dependence of*

- π^0 production in cu+cu collisions at $\sqrt{s_{NN}} = 22.4$, 62.4, and 200 gev, *Physical Review Letters* **101** (oct, 2008) .
- [17] C.-Y. Wong and G. Wilk, *Tsallis fits to p_T spectra for p-p collisions at the lhc*, *Acta Physica Polonica B* **43** (2012) 2047–2054.
- [18] ALICE collaboration, B. Abelev, J. Adam, D. Adamová, A. Adare, M. Aggarwal, G. Aglieri Rinella et al., *Energy dependence of the transverse momentum distributions of charged particles in pp collisions measured by alice*, *The European Physical Journal C* **73** (2013) 1–12.
- [19] S. Acharya, D. Adamová, M. M. Aggarwal, G. A. Rinella, M. Agnello, N. Agrawal et al., *Production of π^0 and η mesons up to high transverse momentum in pp collisions at 2.76 tev*, *The European Physical Journal C* **77** (2017) 1–25.
- [20] ALICE collaboration, S. Acharya, D. Adamová, S. P. Adhya, A. Adler, J. Adolfsson, M. M. Aggarwal et al., *Production of charged pions, kaons, and (anti-)protons in pb-pb and inelastic pp collisions at $\sqrt{s_{NN}} = 5.02$ tev*, *Phys. Rev. C* **101** (Apr, 2020) 044907.
- [21] CMS collaboration, A. M. Sirunyan et al., *Measurement of prompt and nonprompt charmonium suppression in PbPb collisions at 5.02 TeV*, *Eur. Phys. J. C* **78** (2018) 509, [1712.08959].
- [22] A. Sirunyan, A. Tumasyan, W. Adam, F. Ambrogio, E. Asilar, T. Bergauer et al., *Nuclear modification factor of d0 mesons in pbb collisions at $s_{nn}=5.02$ tev*, *Physics Letters B* **782** (2018) 474–496.
- [23] G. Aad, B. Abbott, D. Abbott, A. Abed Abud, K. Abeling, D. Abhayasinghe et al., *Measurement of the nuclear modification factor for muons from charm and bottom hadrons in pb+pb collisions at 5.02 tev with the atlas detector*, *Physics Letters B* **829** (2022) 137077.
- [24] B. Abelev, J. Adam, D. Adamová, A. Adare, M. Aggarwal, G. Aglieri Rinella et al., *Centrality dependence of charged particle production at large transverse momentum in pb–pb collisions at $s_{nn}=2.76$ tev*, *Physics Letters B* **720** (2013) 52–62.
- [25] ALICE collaboration, S. Acharya, F. T.-. Acosta, D. Adamová, J. Adolfsson, M. M. Aggarwal, G. Aglieri Rinella et al., *Neutral pion and η meson production at midrapidity in pb-pb collisions at $\sqrt{s_{NN}} = 2.76$ tev*, *Phys. Rev. C* **98** (Oct, 2018) 044901.
- [26] M. Spousta and B. Cole, *Interpreting single jet measurements in pb+pb collisions at the LHC*, *The European Physical Journal C* **76** (Jan, 2016) .
- [27] R. Baier, Y. L. Dokshitzer, A. H. Mueller and D. Schiff, *Quenching of hadron spectra in media*, *Journal of High Energy Physics* **2001** (2001) 033.
- [28] C. E. Coleman-Smith and B. Muller, *Constituent mass dependence of transport coefficients in a quark-gluon plasma*, 2012.
- [29] A. Buzzatti and M. Gyulassy, *Jet flavor tomography of quark gluon plasmas at rhic and lhc*, *Phys. Rev. Lett.* **108** (Jan, 2012) 022301.
- [30] M. Younus, C. E. Coleman-Smith, S. A. Bass and D. K. Srivastava, *Charm quark energy loss in infinite qcd matter using a parton cascade model*, *Phys. Rev. C* **91** (Feb, 2015) 024912.
- [31] Y. Dokshitzer and D. Kharzeev, *Heavy-quark colorimetry of qcd matter*, *Physics Letters B* **519** (2001) 199–206.
- [32] ALICE collaboration, S. Acharya et al., *Direct observation of the dead-cone effect in quantum chromodynamics*, *Nature* **605** (2022) 440–446, [2106.05713].
- [33] M. Petrovici, A. Lindner, A. Pop, M. Târziľă and I. Berceanu, *Geometrical scaling for energies available at the bnl relativistic heavy ion collider to those at the cern large hadron collider*, *Phys. Rev. C* **98** (Aug, 2018) 024904.